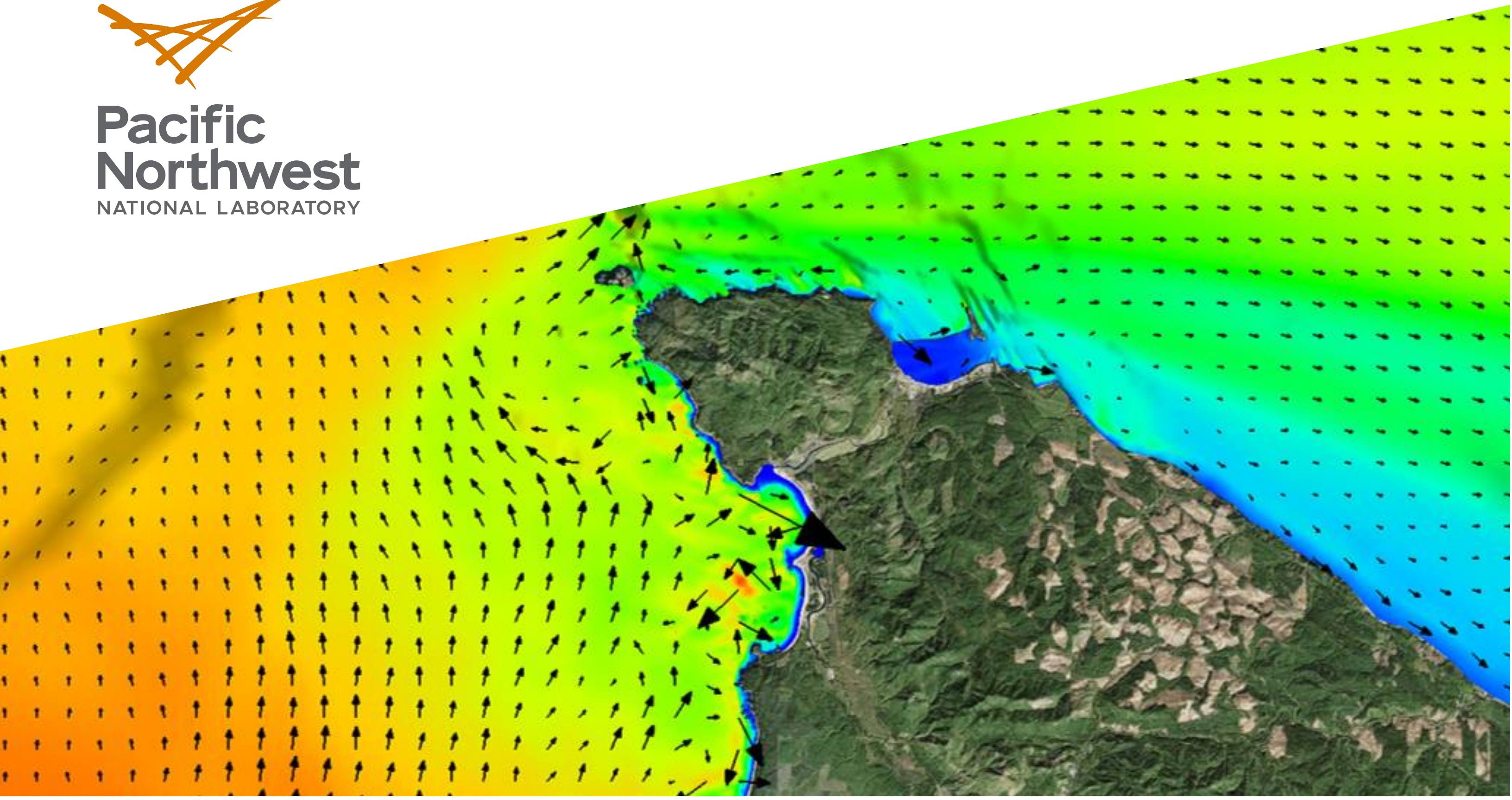

PNNL-32348

# A Multi-variable, Multi-value Hydrodynamic Modeling Approach to Support Marine Energy and Coastal Resilience Applications

October 2021

T Wang
Z Yang
S Geerlofs

U.S. DEPARTMENT OF ENERGY
Prepared for the U.S. Department of Energy
under Contract DE-AC05-76RL01830

PACIFIC NORTHWEST NATIONAL LABORATORY
*operated by*
BATTELLE
*for the*
UNITED STATES DEPARTMENT OF ENERGY
*under Contract DE-AC05-76RL01830*

**Printed in the United States of America**

**Available to DOE and DOE contractors from the**
**Office of Scientific and Technical Information,**
**P.O. Box 62, Oak Ridge, TN 37831-0062;**
**ph: (865) 576-8401**
**fax: (865) 576-5728**
**email: reports@adonis.osti.gov**

**Available to the public from the National Technical Information Service**
**5301 Shawnee Rd., Alexandria, VA 22312**
**ph: (800) 553-NTIS (6847)**
**email: orders@ntis.gov <https://www.ntis.gov/about>**
**Online ordering: http://www.ntis.gov**

PNNL-32348

# A Multi-variable, Multi-value Hydrodynamic Modeling Approach to Support Marine Energy and Coastal Resilience Applications

October 2021

T Wang
Z Yang
S Geerlofs

Prepared for
the U.S. Department of Energy
under Contract DE-AC05-76RL01830

Pacific Northwest National Laboratory
Richland, Washington 99354

# Summary

Funded by the Marine Energy Seedling Laboratory Program, this study aimed to develop a multi-variable, multi-value hydrodynamic modeling approach based on the Finite-Volume Community Ocean Model (FVCOM) to support a wide range of marine renewable energy and coastal resilience applications. We migrated the marine hydrokinetic energy module to simulate tidal energy extraction by tidal turbines under wave-current interactions. We explored the particle tracking module in FVCOM and applied it to Sequim Bay, Washington, to illustrate the surface current field and mimic the pollutant transport near the surface. A tracer-water age module was added to FVCOM to examine water exchange through the entrance. Lastly, a user-specified vertical coordinate option was added to FVCOM to improve simulation of the effect of floating turbines on surface currents and scalar transport.

The above-described model development has been tested using a simplified model domain and demonstrated in real-world coastal systems. The outcome of this project will provide a useful modeling code and approach for marine renewable energy and coastal resilience research and applications.

# Acknowledgments

The project is funded by the U.S. Department of Energy, Office of Energy Efficiency and Renewable Energy, Water Power Technologies Office under Contract DE-AC05-76RL01830 to Pacific Northwest National Laboratory.

# Acronyms and Abbreviations

| | |
|---|---|
| CR | coastal resilience |
| FVCOM | Finite-Volume Community Ocean Model |
| MHK | marine and hydro-kinetic |
| MRE | marine renewable energy |

# Contents

# Figures

## Table

# 1.0 Introduction

Previous modeling studies of marine renewable energy (MRE) resource characterization in U.S. coastal waters have mostly been focused on regional or basin scales, e.g., the U.S. Exclusive Economic Zone (EEZ) and the Salish Sea (Yang et al. 2018, 2021). However, the practical interests of local communities and utility companies are usually at much smaller spatial scales. In addition, despite the potential for MRE to serve as an alternative energy resource to enhance coastal resilience (CR), research on MRE and CR-related applications (e.g., backup power source, shoreline protection, powering seawater desalination) is often loosely connected. Therefore, to better promote and support MRE and CR development, the two subjects need to be addressed together within a single model framework. By addressing MRE and CR together at smaller scales and finer spatial resolutions, it is also possible to provide a refined assessment of associated costs and benefits, which are greatly needed by local communities. For instance, the Makah Tribe located on the northwestern tip of the Olympic Peninsula is an isolated coastal community being threatened by water shortage, tsunami inundation, power loss, and coastal erosion[1]. The Tribe's proximity to MRE resources and strong interest in using MRE to meet their CR needs make their location a great case study site for MRE and CR research and applications (Figure 1).

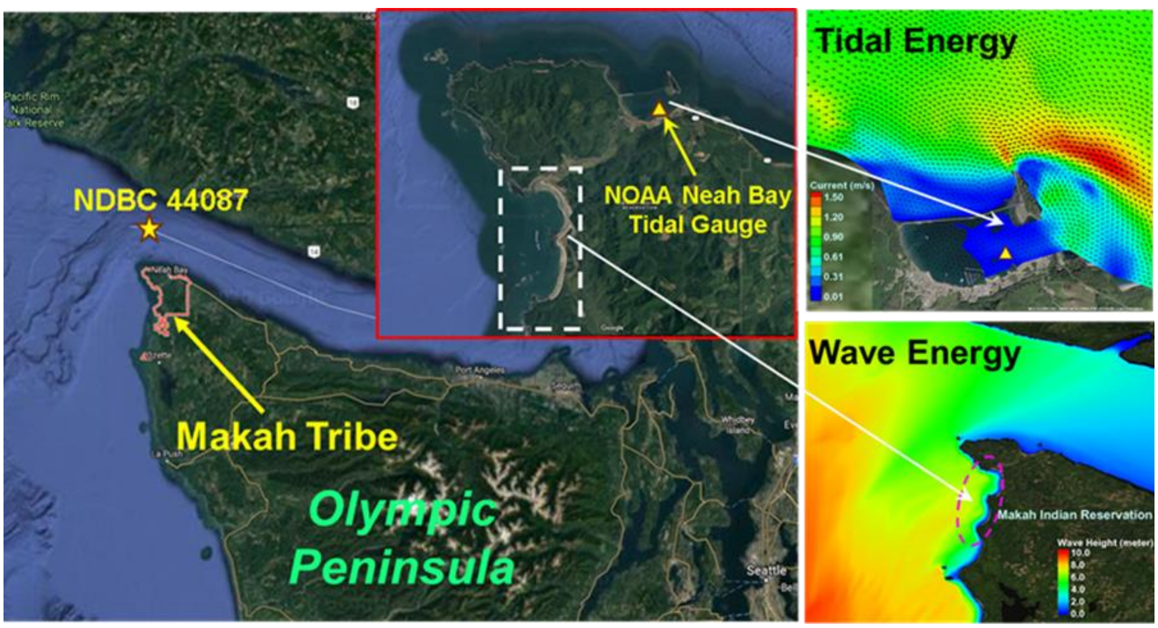


Figure 1. Makah Tribe Reservation on the Olympic Peninsula. The National Oceanic and Atmospheric Administration (NOAA) Neah Bay tidal gauge and National Data Buoy Center (NDBC) Buoy 44087 are both located near Neah Bay (left panel). The right panels show the instantaneous tidal current (upper-right panel) and wind wave height (lower-right panel) distributions from Pacific Northwest National Laboratory's (PNNL) standalone tidal and wave model simulations using FVCOM and Simulating Waves Nearshore (SWAN), respectively.

Based on PNNL's existing MRE and CR research, including wave and tidal energy resource characterization (Wang and Yang 2020; Yang et al. 2021) and storm surge/coastal inundation modeling (Yang et al. 2014, 2020), this study aims to develop a multi-variable, multi-value

[1] https://www.congress.gov/116/meeting/house/110377/witnesses/HHRG-116-AP06-Wstate-GreeneT-20200211.pdf

modeling approach based on the Finite-Volume Community Ocean Model (FVCOM; Chen et al. 2003, 2006). Specific objectives include the following:

- Migrate the marine and hydrokinetic (MHK) module that was developed in an earlier version of FVCOM into the most recent version to simulate tidal stream energy extraction under wave-current interaction conditions.
- Identify and explore new process modules in FVCOM that are related to MRE and CR applications.
- Make addition(s) and improvement to the FVCOM framework for MRE and CR applications.

# 2.0 Methodology

We identified the following tasks that are closely related to MRE and CR applications and are also achievable in this Phase 1 seedling project:

1. Migrate the MHK module from FVCOM v2.7.1 to FVCOM v4.3.1.
2. Explore the particle tracking and sediment transport modules in FVCOM.
3. Add a tracer-water age module and a user-specified vertical coordinate option to FVCOM.
4. Test the above modules using a simplified prototype model domain and/or realistic coastal sites.

## 2.1 MHK Module Migration and Testing

A MHK module was developed within FVCOM v2.7.1 to explicitly simulate tidal stream energy extraction by turbines (Yang et al. 2013). This module has been validated against analytical solutions and laboratory experiments (Wang et al. 2014). It was subsequently used for characterizing the tidal energy resource and assessing the hydrodynamic impact of tidal energy extraction in several tidal energy hotspots in the U.S. (Yang et al. 2014, 2021; Wang and Yang 2020). However, FVCOM v2.7.1 does not consider wave-current interactions, which can be important in coastal waters with high tidal and wave energy potential, such as Neah Bay, Washington. Wave-current interaction has been implemented in FVCOM since v3. Under the task reported on here, we migrated the MHK module into the most recent FVCOM version (v4.3.1).

## 2.2 Exploration of Sediment Transport and Particle Tracking Modules

FVCOM has built-in sediment transport and particle tracking modules. The sediment module simulates the change in sediment bed and shoreline morphology, which is closely related to CR. The particle trajectory module simulates material transport using the Lagrangian particle tracking method, which is particularly applicable to particulate matter such as larvae and marine debris (e.g., plastic wastes). It is thus useful to explore these two modules in FVCOM.

## 2.3 Development of a Dye-Water Age Module and a User-Specified Vertical Coordinate Option

Simulating dye (tracer) using a hydrodynamic model is a very popular way to illustrate scalar transport in coastal systems. Certain biological and/or chemical properties also can be assigned to the tracer to represent various contaminants such as fecal bacteria. The built-in dye module in FVCOM does not have completed open and rivers boundary conditions, which limits its practical applications. Under this task, we implemented a separate tracer module with proper boundary conditions referenced to schemes used for salinity and temperature simulations. We further expanded the module with two tracers so that it can be used to calculate the mean water age (or age of water) using the two-tracer approach that was first described by Deleersnijder et al. (2001) and has been later used in many other studies. The tracer-water age module was first implemented in v2.7.1 and will be migrated into v4.3.1 in the future.

The default vertical coordinate in FVCOM is a terrain-following sigma stretch coordinate. Hence, the absolute thickness of the surface layers at each element could vary substantially as a function of the total water depth. This could cause challenges in simulating freshwater plume or pollutants that tend to stay near the surface. FVCOM also has a hybrid vertical coordinate option that combines the strength of Z and sigma coordinates to overcome this limitation, but users need to carefully determine the input parameter values in advance. In this task, by referencing to the hybrid coordinate option, we added a relatively more convenient, user-specified vertical coordinate option so that a hybrid coordinate could be constructed more easily.

## 2.4 A Simplified Model Domain for Model Testing

A simplified computational domain was constructed for model testing (Figure 2). This domain consists of a semi-circular coastal ocean, a narrow entrance/inlet connecting the ocean to a tidal basin, and a tidal river/estuary discharging into the upper end of the basin. For computational efficiency, the grid resolution remains relatively coarse with side length varying from ~250 m in the inlet and river to ~2,000 m at the ocean boundary. The grid consists of a total of 2,644 triangular elements and 1,416 vertices. Ten uniform sigma layers were used for all runs except Run 6, in which a user-specified hybrid vertical coordinate was used. Depending on specific model runs, various forcing mechanisms (e.g., open boundary tides and waves, surface wind forcing, river input) were turned on or off. In all test runs, the Coriolis force effect was not considered.

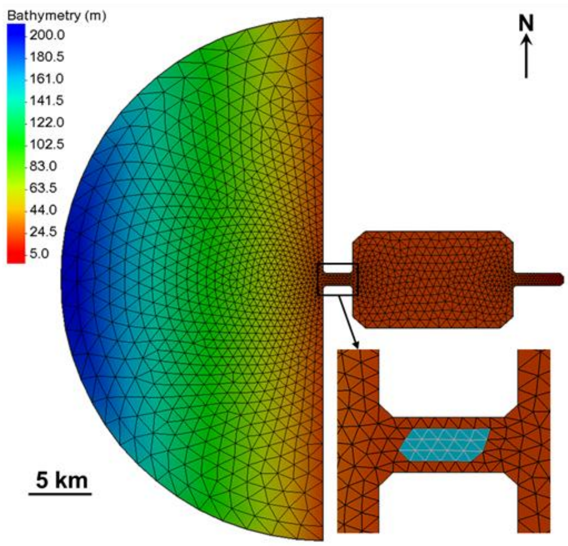


Figure 2. A simplified model domain consisting of a semi-circular coastal ocean, inlet, bay, and river. The inset is a zoom-in view of the inlet area, and the highlighted elements indicated the location of the tidal turbine farm.

Table 1 lists the model test runs conducted using the simplified model domain.

Table 2 lists the model applications to real-world coastal sites.

Table 1. List of model test runs using the simplified model domain.

| Run# | Description | Tidal Boundary | Wave Boundary | Meteorological Forcing | River Input |
|---|---|---|---|---|---|
| 1 | Wave-current interaction with waves and tides | Yes | Yes | Yes | No |
| 2 | Wave-current interaction with waves only (no tides) | No | Yes | Yes | No |
| 3 | Wave-current interaction with waves and tides + tidal turbine farm | Yes | Yes | Yes | No |
| 4 | Wave-current interaction with tides and waves + sediment | Yes | Yes | Yes | No |
| 5 | Dye-water age simulation with default vertical sigma coordinate | Yes | No | Yes | Yes |
| 6 | Dye-water age simulation with user-specified vertical coordinate | Yes | No | Yes | Yes |

Table 2. List of model test runs using realistic coastal sites.

| Run# | Description | Study Site | Tidal Boundary | Wave Boundary | Meteorological Forcing | River Input |
|---|---|---|---|---|---|---|
| 7 | Particle trajectory simulation | Sequim Bay | Yes | No | No | No |
| 8 | Storm surge and salinity simulation using user-specified vertical coordinate | Delaware Bay | Yes | No | Yes | Yes |
| 9 | Dye-water age simulation with user-specified vertical coordinate | Hood Canal | Yes | No | Yes | Yes |
| 10 | Wave-current interaction with waves and tides | Neah Bay | Yes | Yes | Yes | No |

# 3.0 Results and Discussion

The following sections describe the model development and testing using the simplified model domain and applications to realistic coastal sites.

## 3.1 MHK Module Testing under Wave-Current Interaction Conditions

Figure 3 shows the coupled wave-current simulation results by FVCOM v4.3.1. Figure 3a-c shows instantaneous wind, surface elevation, and surface current fields for the wave-current interaction case (Run 1). Figure 3d shows the surface current field for Run 2, in which the prescribed open boundary tidal elevations in Run 1 were replaced with constant, zero surface elevations. Figure 4 is a close-up view of the instantaneous surface current field. The results suggest that surface currents in the coastal ocean are driven by the combination of wind forcing and open boundary tides (Figure 3). In comparison, surface currents inside the inlet are mostly controlled by open boundary tides (Figure 4a, b).

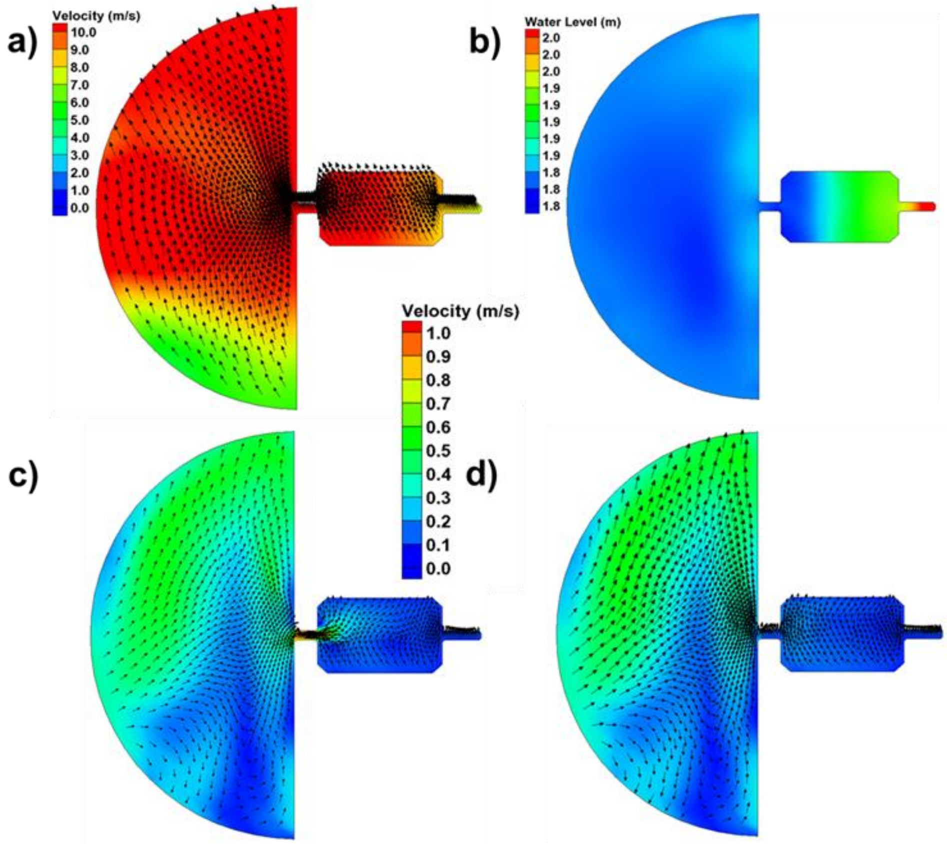


Figure 3. Instantaneous distribution of (a) surface wind field, (b) water surface elevation, and (c) surface currents during the flood tide for Run 1; (d) shows the instantaneous distribution of surface current field for Run 2.

Figure 4b, c show the impact of tidal turbine farm deployed in the surface layer of the inlet on the surface currents, i.e., the current speed is reduced by the presence of the turbine farm.

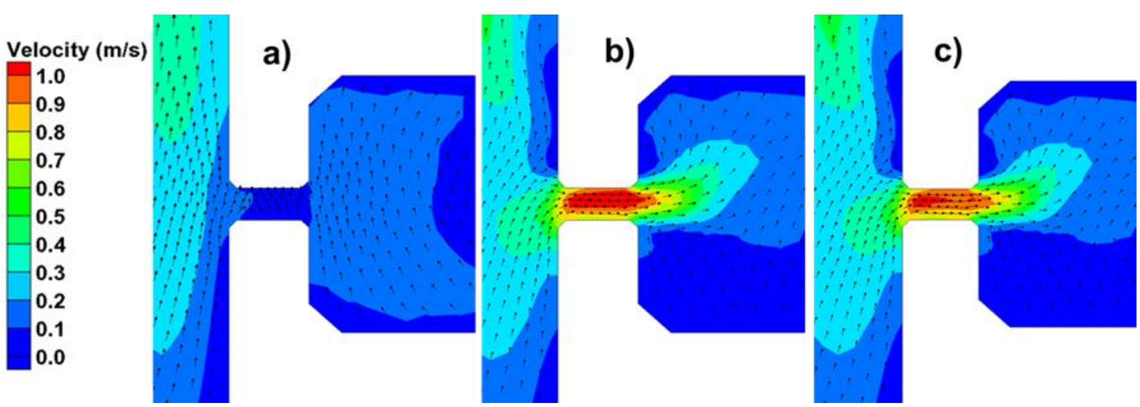


Figure 4. Zoom-in view of the instantaneous distribution of surface current field for (a) Run 2, (b) Run 1, and (c) Run 3.

Figure 5 shows the instantaneous significant wave height comparison between Runs 1 and 2. The difference is very small throughout the model domain except at the entrance of the inlet and on the northwest corner of the bay, which is presumably due to stronger wave-current interactions at these locations.

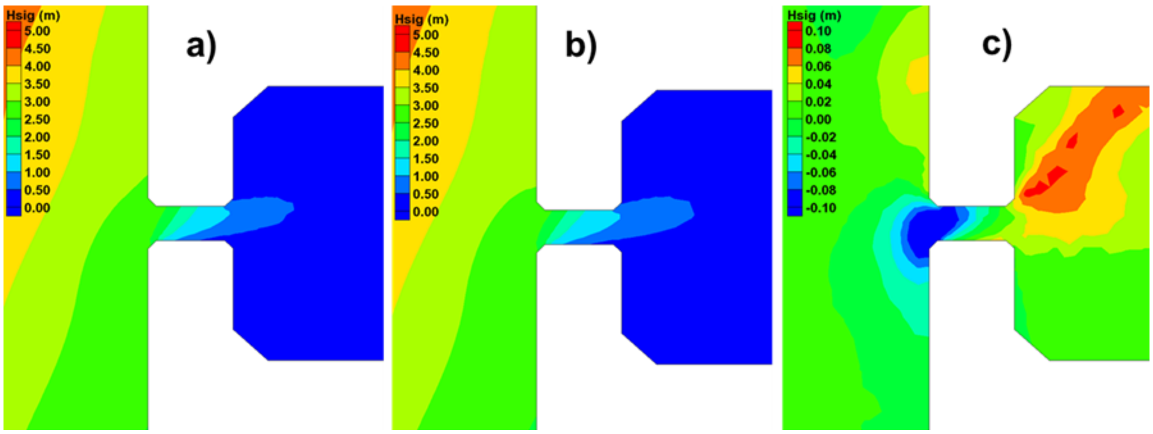


Figure 5. Instantaneous distribution of significant wave height during flood tide for (a) Run 2, (b) Run 1, and (c) difference between Runs 1 and 2 (Run 1 minus 2).

Figure 6 shows the extracted power time series by the hypothetical tidal farm over a few tidal cycles. The power varies substantially depending on the tidal stage.

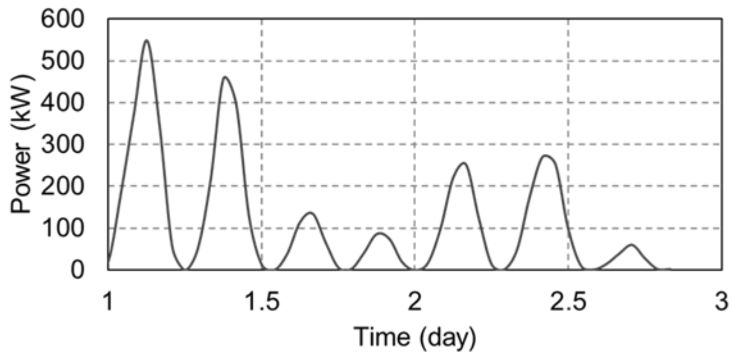


Figure 6. Time series of extracted tidal power by the turbine farm in Run 3.

## 3.2 Exploration of the Sediment Transport Module

FVCOM has a few built-in options to simulate sediment transport, which needs further exploration and testing. Under this task, we explored the very basic sediment module for non-cohesive sediment transport (e.g., sand). Figure 7 is a snapshot of the depth-averaged sediment concentration after 60 hours of simulation with a uniform initial condition of 100 mg/L. After 60 hours of model simulation, the depth-averaged sediment concentration generally follows the depth contour, suggesting settling plays an important role in reducing suspended sediment concentrations in the water column.

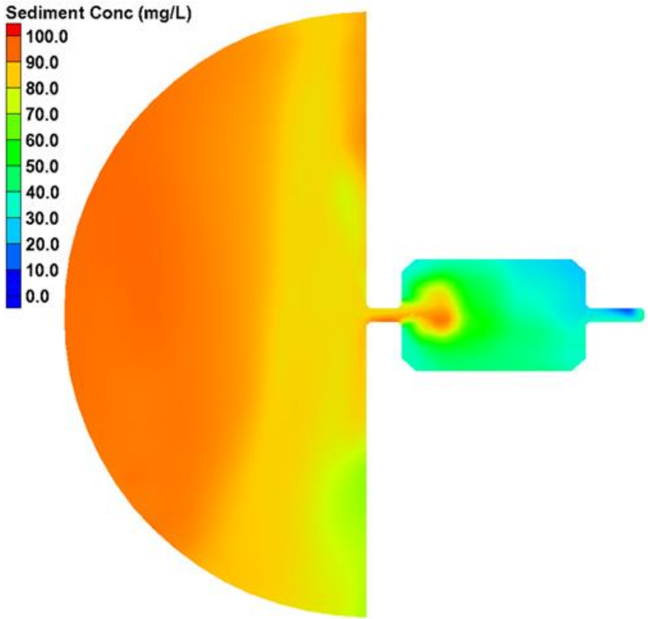


Figure 7. Instantaneous depth-averaged sediment concentration distribution after 60 hours of simulation during Run 4.

## 3.3 Exploration of the Particle Tracking Module

After finishing the initial testing of the particle tracking module using the simplified model domain, we applied the module to Sequim Bay, Washington, to illustrate tidal circulations. Figure 8 compares surface particle distributions between the initial release and after 2 days of model simulation. At the end of the 2-day simulation, the particle locations are much different than their initial locations and spread into patches across the model domain. The spatial pattern is a good indication of the current field, e.g., the presence of tidal eddies both inside and outside of Sequim Bay.

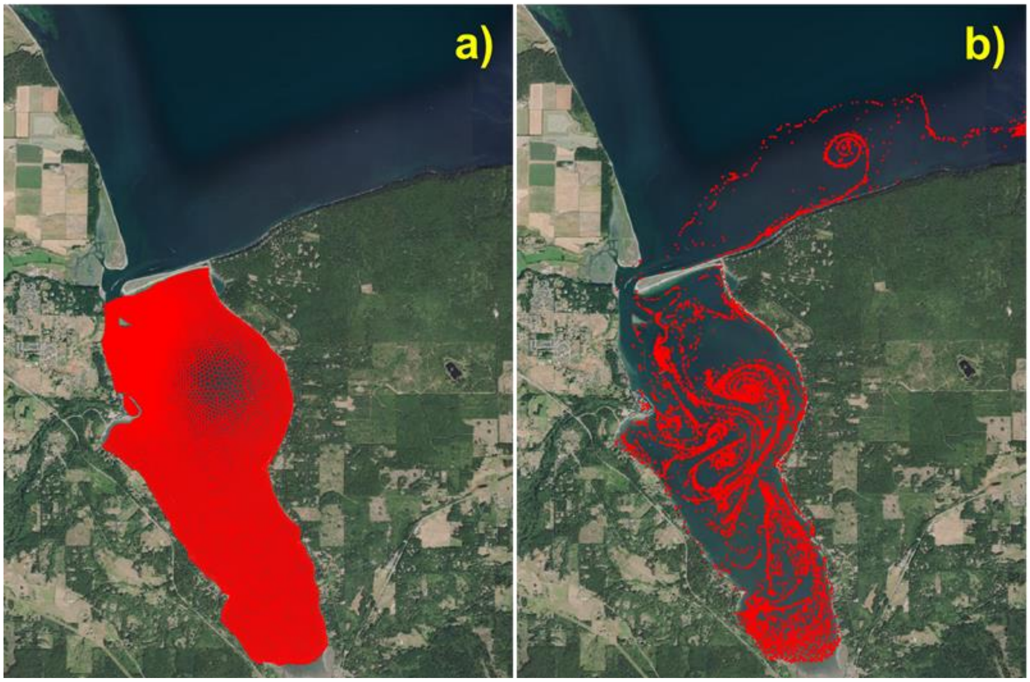


Figure 8. Instantaneous particle distributions for (a) the initial condition and (b) after 2 days of model simulation in Run 7.

Figure 9 shows selected particle trajectories over 6 days of model simulation. For individual particles, their trajectories are highly dependent upon on their initial release locations. For instance, in Figure 9a, the particle released near the inlet was quickly flushed out of model domain within the first couple days. In comparison, in Figure 9f, the particle released in the upper bay remains, surrounding its initial location after 6 days, indicating the generally weaker tidal exchange in the upper bay. Particle trajectories in Figure 9b-e confirm the strong presence of tidal eddies, especially in the middle of Sequim Bay.

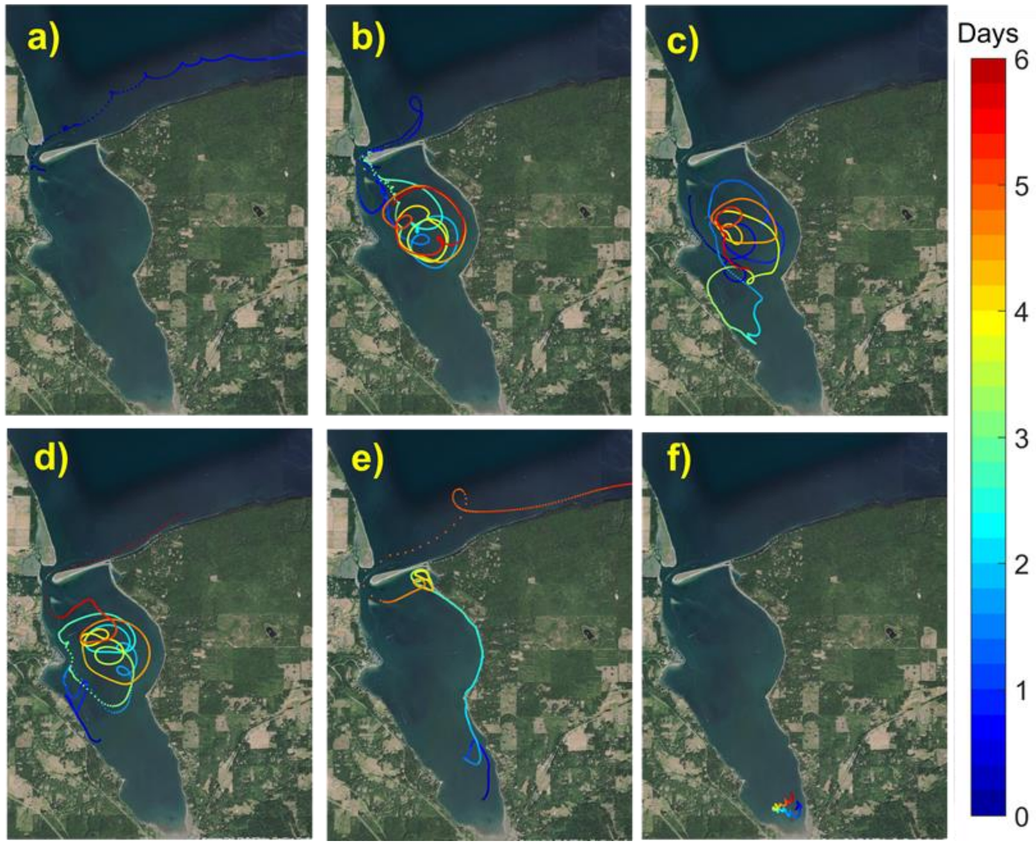


Figure 9. Selected particle trajectories over the course of 6 days of model simulation.

## 3.4 Development of a User-Specified Vertical Coordinate Option

Figure 10 shows a comparison of the vertical layer distribution for the default sigma coordinate and the newly added user-specified hybrid coordinate option. This example shows that by using the user-specified hybrid coordinate, higher-resolution, Z-coordinate type of depth layers can be constructed to improve the representation of surface processes.

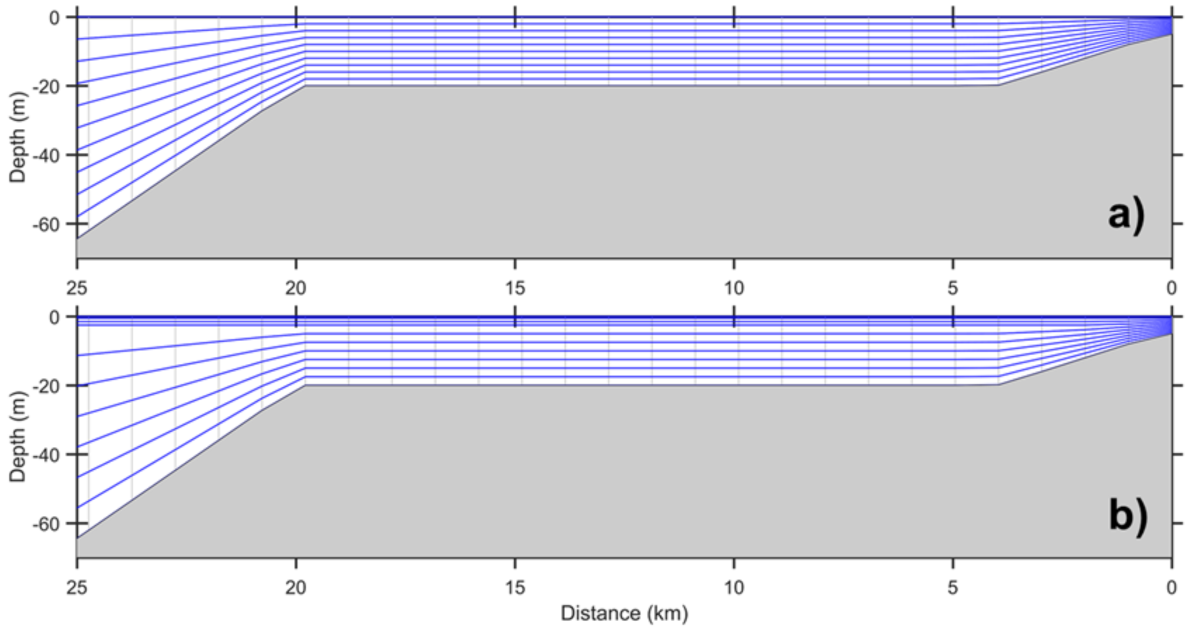


Figure 10. (a) Vertical layer distribution for the default, terrain-following sigma coordinate and (b) user-specified layer thickness option to allow for higher-resolution, near constant layer thickness distributions at surface layers.

Figure 11 compares the instantaneous surface salinity field between the model runs using the default sigma coordinate (Run 5) and user-specified hybrid coordinate (Run 6). After two months of simulation, surface salinity distribution is substantially different between these two runs. For instance, the user-specified hybrid coordinate appears to produce a more resolved coastal plume outside of the tidal inlet.

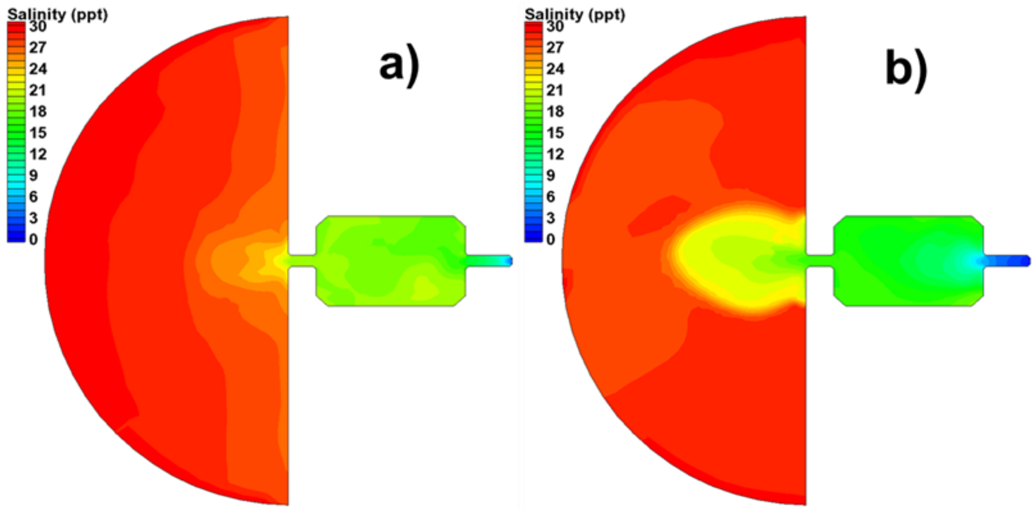


Figure 11. Instataneous surface salinity field for (a) the default sigma coordinate and (b) the user-specified layer thickness option after 2 months of model simulation during Runs 5 and 6, respectively.

Figure 12 shows the user-specified vertical coordinate option was applied to simulate storm surge and salinity in Delaware Bay during Hurricane Irene (2011). Although more model validations with field measurements need to be conducted, this demonstrates that the new hybrid coordinate option can be applied to real-world sites, especially for improvement in simulating the effects of free-floating tidal turbines on the surface transport process.

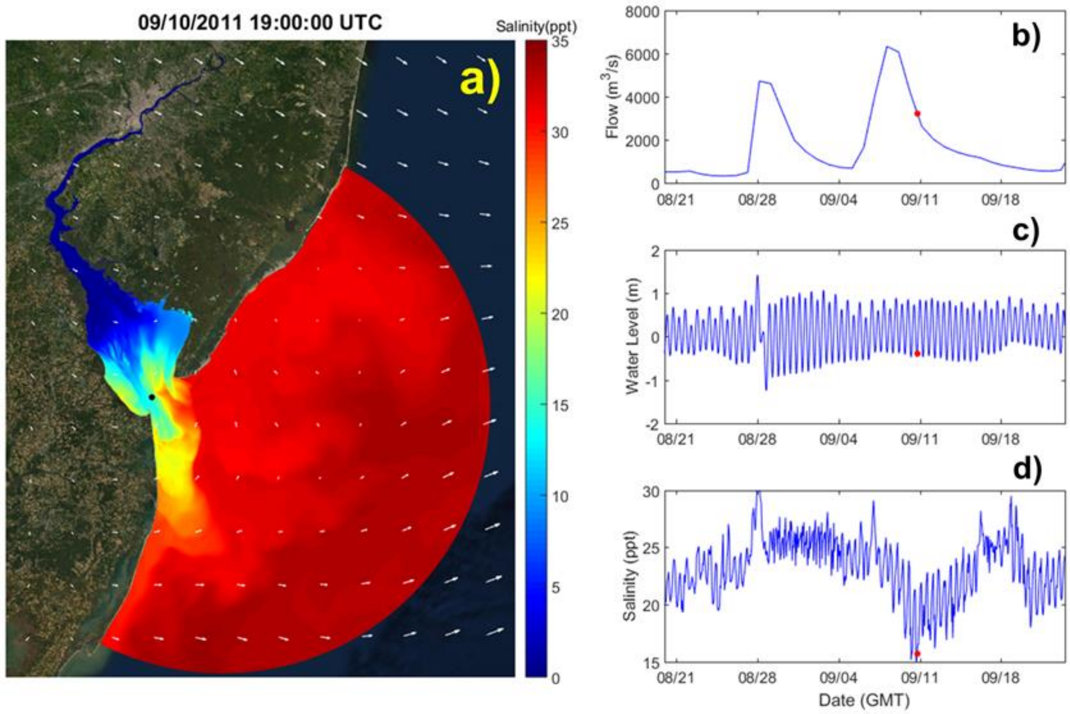


Figure 12. Implementation of the user-specified vertical coordinate option to simulate storm surge and salinity during Hurricane Irene (2011) in Delaware Bay (Run 8). (a) instantaneous surface salinity field, (b) river input, (c) surface elevation, and (d) salinity time series near the mouth of Delaware Bay.

## 3.5 Development of a Tracer-Water Age Module

The dye-water age module was tested using the simplified model domain for both the default sigma and user-specified hybrid coordinate options (Runs 5 and 6). In these simulations, a constant dye concentration of 100 mg/L was released from the river upstream. After 2 months of model simulations, the dye plume reaches the coastal ocean in both cases (Figure 13a, b). However, the dye plume reaches the open boundary more effectively by using the user-specified hybrid coordinate (Figure 13c, d). The mean water age distribution also confirms that it took less time for freshwater to reach the open boundary.

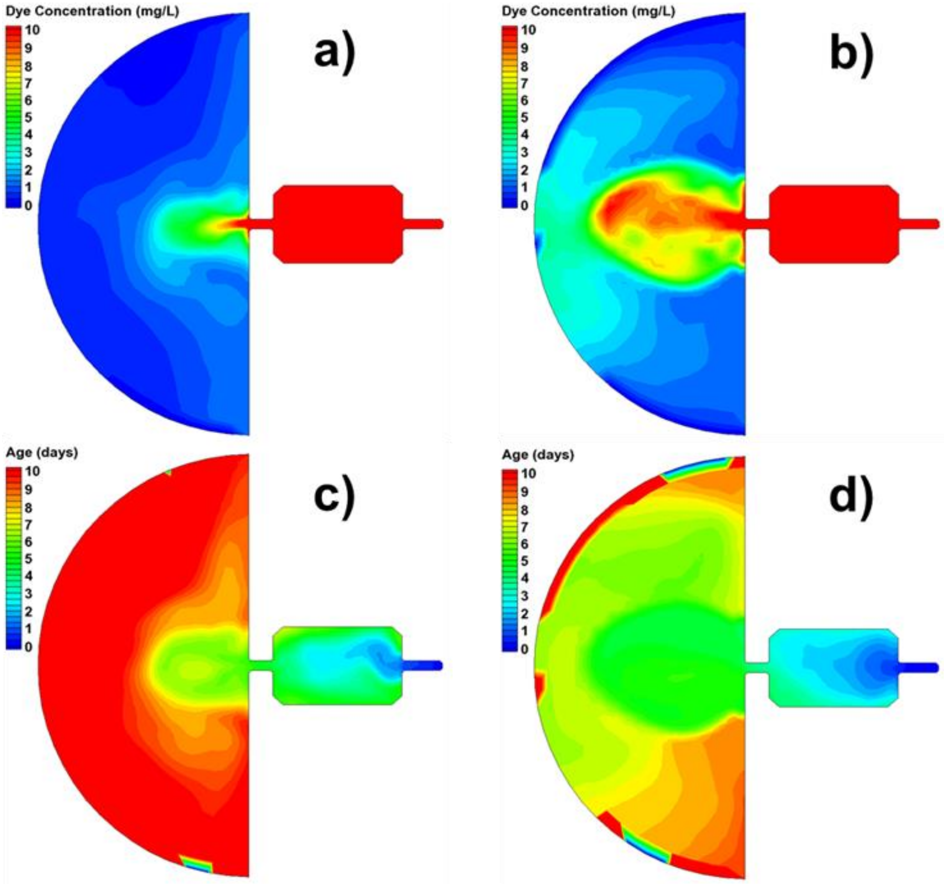


Figure 13. Instantaneous tracer/dye concentration field at the surface layer for the (a) default sigma coordinate and (b) user-specified vertical coordinate options; (c) and (d) are the corresponding mean water age distributions after 2 months of model simulations for these two vertical coordinate options (Runs 5 and 6, respectively).

The dye-water age module was further applied to understand water exchange through the entrance of Hood Canal, Washington (Run 9). A constant dye concentration of 10 mg/L was specified at the open boundary instead of at the river boundaries. Thus, water age in this case represents the average time for saltier, oceanic water to arrive at different areas in Hood Canal through its entrance. Figure 14 shows the instantaneous dye concentration and mean water age field for the surface and bottom layers after 2 months of model simulations. The results show that the saltwater (indicated by dye concentrations) intrudes into Hood Canal mainly through the bottom. Consequently, it took less time (i.e., shorter water age) to arrive at different locations in Hood Canal.

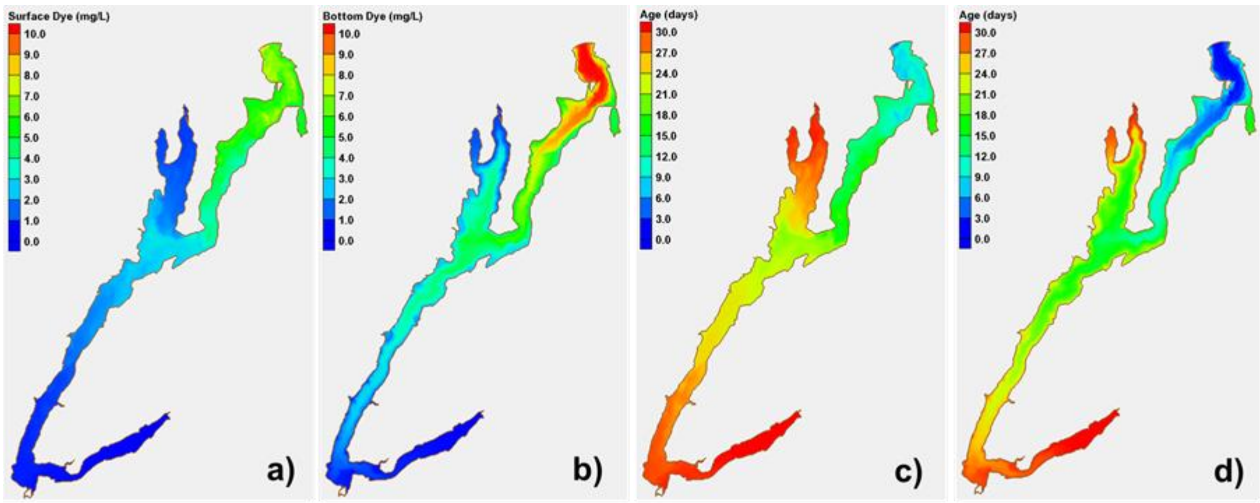


Figure 14. Instataneous tracer/dye distribution in Hood Canal for the (a) surface and (b) bottom layers and the corresponding mean water age distribution at the (c) surface and (d) bottom layers after 2 months of simulations.

## 3.6 Preliminary Application to Neah Bay, Washington

Lastly, the updated FVCOM v4.3.1 model framework was applied to Neah Bay to simulate wave-current interaction under realistic meteorological, tidal, and wave forcing conditions. Figure 15 shows the computational grid that covers the entire Salish Sea with much more refined resolution for the Neah Bay area. Inside Neah Bay and at the shorelines around the Makah Tribe Reservation, the grid resolution remains as fine as 40 m.

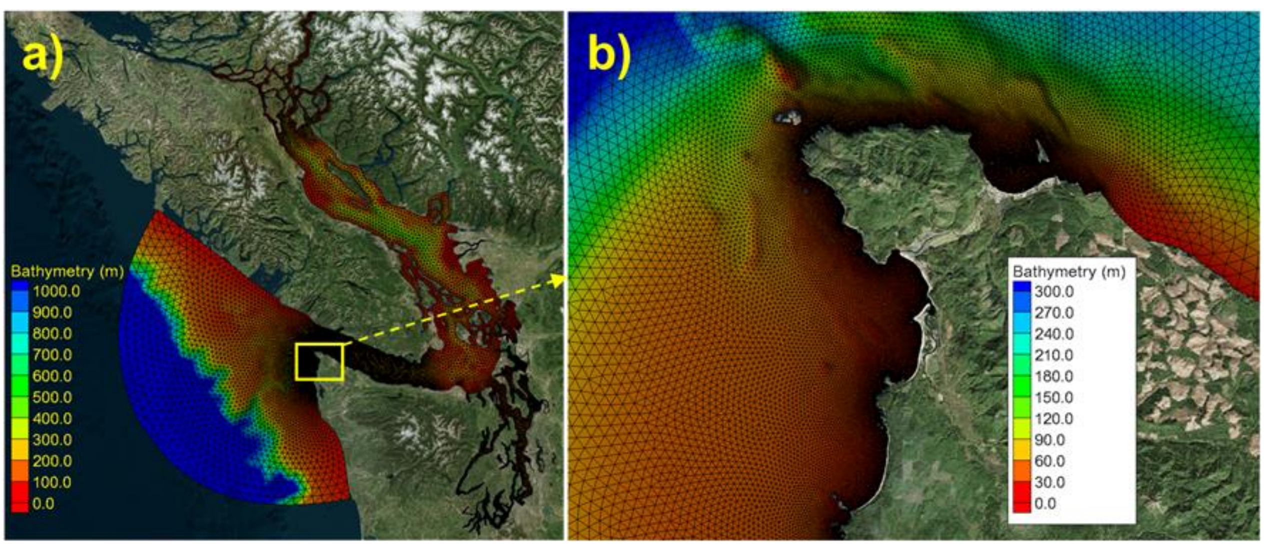


Figure 15. The model grid used for the Neah Bay study site to study wave-current interaction (Run 10).

Figure 16 shows model-predicted instantaneous depth-averaged current field and significant wave height distribution. High currents can be seen near the shorelines of the Makah Indian Reservation (Figure 16a). The wave height is largely reduced as waves propagate into the Strait of Juan de Fuca from the Pacific Ocean (Figure 16b). Inside Neah Bay, both currents and waves are much reduced because of its location and the presence of the north jetty.

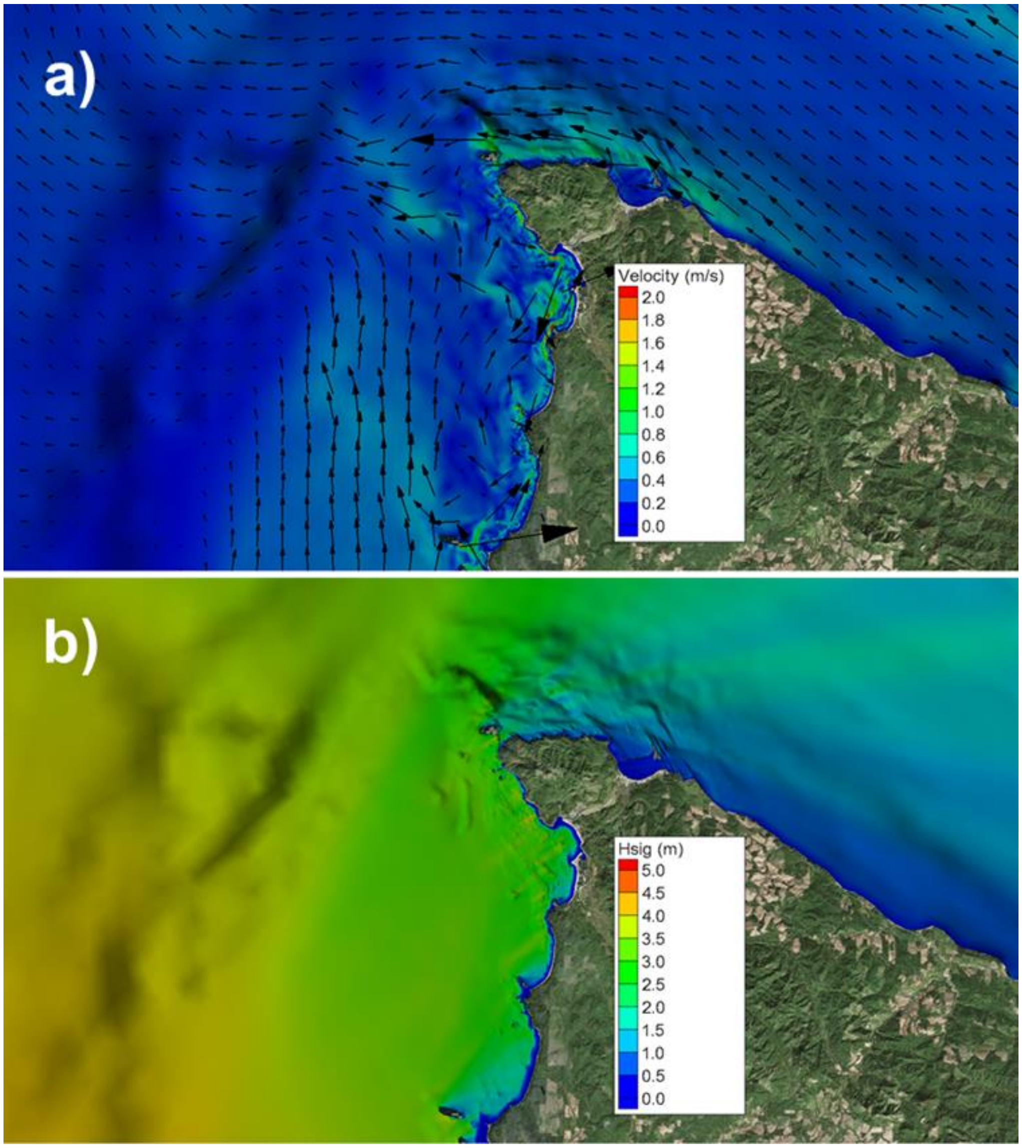


Figure 16. (a) Instantaneous surface current field and (b) significant wave height at 11/31/2015 6:00 AM (GMT) simulated by FVCOM v4.3.1.

# 4.0 Conclusion

In this study, we migrated the MHK module from an earlier version of FVCOM (v2.7.1) into the most recent version (v4.3.1) to simulate tidal energy extraction by tidal turbines under wave-current interaction conditions. The same model can be readily applied to address coastal inundation and flooding caused by episodic events, such as storms and tsunamis. Hence, this approach already has broad applicability to support MRE and CR research and development, especially for remote coastal communities under the Energy Transitions Initiative Partnership Project.

We further explored and added a few additional modules to FVCOM. These modules have been tested using a simplified computational domain and preliminarily applied to various real-world coastal sites. These new capabilities can be used to support research related to circulation (e.g., flushing rate), biology and fishery (e.g., larvae transport), and fate and transport of pollutants (e.g., plastic debris, fecal bacteria, brine discharge). We envision that with some further development and testing of the current approach, we can use it as a predictive tool to support the Power the Blue Economy applications.

For the next step, we expect to apply the approach to one or more case-study sites (e.g., Neah Bay, Washington/Makah Tribe Reservation) that have immediate needs for MRE and CR research and development. For example, we can conduct a much more refined tidal and wave energy resource assessment around the Neah Bay/Makah Tribe Reservation coast, which is much needed by the MRE industry. Using tracer as the proxy, we can conduct additional modeling assessments of the potential hydrodynamic and environmental impacts resulting from energy extraction. Lastly, we hope to continue improving the modeling approach to make it an even more useful tool to support broader MRE and CR applications.

# 5.0 References

Chen C, H Liu, and R Beardsley. 2003. An unstructured grid, finite-volume, three-dimensional, primitive equations ocean model: application to coastal ocean and estuaries. *Journal of Atmospheric and Oceanic Technology* 20: 159-186.

Chen C, R Beardsley, and G Cowles. 2006. An unstructured grid, finite-volume coastal ocean model (FVCOM) system. *Oceanography* 19: 78-89.

Deleersnijder E., J-M Campin, and EJM Delhez. 2001. The concept of age in marine modelling: I. Theory and preliminary model results. *Journal of Marine Systems* 28: 229–267.

Wang T, T Khangaonkar, W Long, and G Gill. 2014. Development of a Kelp-Type Structure Module in a Coastal Ocean Model to Assess the Hydrodynamic Impact of Seawater Uranium Extraction Technology. *Journal of Marine Science and Engineering* 2, 81–92.

Wang T. and Z Yang. 2020. A tidal hydrodynamic model for Cook inlet, Alaska, to support tidal energy resource characterization. *Journal of Marine Science and Engineering* 8(4).

Yang Z, T Wang, R Leung, K Hibbard, T Janetos, I Kraucunas, J Rice, B Preston, and T Wilbanks. 2014. A modeling study of coastal inundation induced by storm surge, sea-level rise, and subsidence in the Gulf of Mexico. 71: 1771-1794.

Yang Z, T Wang, and AE Copping. 2013. Modeling tidal stream energy extraction and its effects on transport processes in a tidal channel and bay system using a three-dimensional coastal ocean model. *Renewable Energy* 50, 605–613.

Yang Z, T Wang, A Copping, and S Geerlofs. 2014. Modeling of in-stream tidal energy development and its potential effects in Tacoma Narrows, Washington, USA. *Ocean & Coastal Management* 99, 52–62.

Yang Z, W Wu, T Wang, and L Castrucci. 2018. *High-Resolution Regional Wave Hindcast for the U.S. West Coast*. PNNL-28107, Pacific Northwest National Laboratory, Richland, Washington.

Yang Z, T Wang, RA Branch, Z Xiao, and M Deb. 2021. Tidal Stream Energy Resource Characterization in the Salish Sea. *Renewable Energy* 172: 188-208.

Yang Z, T Wang, L Castrucci, and I Miller. 2020. Modeling assessment of storm surge in the Salish Sea. *Estuarine, Coast, and Shelf Science* 238.

PNNL-32348


**Pacific Northwest National Laboratory**

902 Battelle Boulevard
P.O. Box 999
Richland, WA 99354
1-888-375-PNNL (7665)

***www.pnnl.gov***